HHS Public Access

Author manuscript

Alzheimers Dement. Author manuscript; available in PMC 2023 September 28.

Published in final edited form as:

Alzheimers Dement. 2023 August ; 19(8): 3389–3405. doi:10.1002/alz.12960.

Identification of circRNAs Linked to Alzheimer's Disease and Related Dementias

Sambhavi Puri[1,2,*], **Junming Hu**[3,*], **Zhuorui Sun**[3], **Mintao Lin**[3], **Thor D. Stein**[4,8,9,10], **Lindsay A. Farrer**[2,3,5,6,7,8,9], **Benjamin Wolozin**[1,2,#], **Xiaoling Zhang**[3,6,9,#]

[1]Department of Pharmacology & Experimental Therapeutics, Boston University School of Medicine, Boston, MA, USA

[2]Department of Neurology, Boston University School of Medicine, Boston, MA, USA

[3]Department of Medicine (Biomedical Genetics), Boston University School of Medicine, Boston, MA, USA

[4]Department of Pathology and Laboratory Medicine, Boston University School of Medicine, Boston, MA, USA

[5]Department of Ophthalmology, Boston University School of Medicine, Boston, MA, USA

[6]Department of Biostatistics, Boston University School of Public Health, Boston, MA, USA

[7]Department of Epidemiology, Boston University School of Public Health, Boston, MA, USA

[8]Alzheimer's Disease Research Center, Boston University School of Medicine, Boston, MA, USA

[9]Framingham Heart Study, Boston University School of Medicine, Framingham, MA, USA

[10]VA Boston Healthcare System, Boston, MA, USA

Abstract

INTRODUCTION: CircRNAs exhibit selective expression in the brain and differential regulation in Alzheimer's disease (AD). In order to explore the role of circRNA in AD, we investigated how circRNA expression varies between brain regions and with AD-related stress in human neuronal precursor cells (NPCs).

METHODS: Ribosomal RNA-depleted hippocampus RNA-sequencing data were generated. Differentially regulated circRNAs in AD and related dementias were detected using CIRCexplorer3 and limma. circRNA results were validated using RT-qPCR of cDNA from the brain and NPCs.

RESULTS: We identified 48 circRNA significantly associated with AD. We observed that circRNA expression differed by dementia subtype. Using NPCs, we demonstrated that exposure to oligomeric tau elicits downregulation of circRNA similar to that observed in the AD brain.

[#]Corresponding authors: *Dr. Benjamin Wolozin, Boston University School of Medicine, Pharmacology & Experimental Therapeutics, R-614, 72 East Concord Street, Boston, MA 02118; (617) 358-1995;* bwolozin@bu.edu; *Dr. Xiaoling Zhang, Boston University School of Medicine, Biomedical Genetics E223, 72 East Concord Street, Boston, MA 02118; (617) 358-3580;* zhangxl@bu.edu.
[*]These authors contributed equally to this work

DISCUSSION: Our study shows that differential expression of circRNA can vary by dementia subtype and brain region. We also demonstrated circRNAs can be regulated by AD-linked neuronal stress independently from their cognate linear mRNAs.

Keywords

circular RNA; oligomeric tau toxicity; Alzheimer disease; Lewy body disease; vascular dementia; neuronal precursor cells

Introduction

Late-onset Alzheimer's disease (AD) is a complex neurodegenerative disorder that is the most common cause of dementia. Recent genomic studies have discovered thousands of well-expressed, stable circular RNAs (circRNAs) [1]. These circRNAs are produced from both protein-coding genes and non-coding regions of the genome via a process known as back-splicing [2–4]. CircRNAs are more enriched in neuronal tissues and are often derived from genes specific for neuronal and synaptic function [3, 5–7]. The discovery of circRNAs opens an entirely new window into mechanisms of neurodegeneration in Alzheimer's disease (AD) and related dementia (ADRD).

CircRNAs could contribute to neurodegeneration by acting as sponges that sequester microRNA and RNA-binding proteins (RBPs) away from normal mRNA targets, altering the splicing or expression of target mRNAs [8]. RBPs also regulate circRNA production by binding to the flanking intronic sequences of circRNAs, which contain many conserved binding sites of splicing factors/RBPs [9–11]. Many RBPs become sequestered in protein aggregates in AD, which could cause dysfunctional regulation of circRNAs. Studies from the field of oncology suggest that differential expression of circRNAs causes wide-ranging effects on tumor biology [12]. Biomarker studies of circRNA also demonstrate multiple examples of associations with tumor levels, type, prognosis, or therapeutic response.

The expression pattern of circRNA in AD is only beginning to be studied [1]. Studies have begun to characterize circRNA expression in AD brain and mouse models of AD [13,14]. However, numerous critical questions remain. Methods for detecting circRNA are evolving, the effects of disease heterogeneity on circRNA expression are poorly understood, and comparisons between brain regions and the regulation of circRNA by AD-related factors in human neurons are unexplored. Thus, the field of circRNA presents a major unexplored avenue of RNA metabolism that demands investigation to expand our understanding of AD mechanisms.

In this study, we conducted a circular-transcriptome-wide analysis and examined circRNA expression patterns associated with AD and clinical and neuropathological AD severity measures in human hippocampus and cortex brain regions. We validate prior studies of circRNA in the AD cortex and demonstrate novel patterns of expression in the AD hippocampus. We show changes in the expression of predicted mRNA targets for AD-associated circRNA. We also show that circRNA expression differs by dementia subtype. We demonstrate robust circRNA expression in human neuronal precursor cells (NPCs). Using

NPCs to study qPCR validated circRNA, we show that exposure to oligomeric tau elicits downregulation of circRNA similar to that observed in AD brain.

Results

Study design/Subject Characteristics

The study design included calling and quantifying circRNA in two brain regions from three study cohorts in which independent RNA-seq datasets were derived from neuropathologically confirmed AD cases and control brain tissues. In the hippocampus dataset, 210 individuals were assessed at the ADRC of Boston University School of Medicine, and their demographic, clinical severity and neuropathological information are presented in Table 1. Out of 210 BU ADRC participants, 207 European ancestry individuals remained for inclusion in the analysis. These include 79 Pure AD cases, 56 AD cases with Vascular Dementia and 47 AD cases with Lewy body dementia (LBD) and 21 cognitively normal controls. Pure AD was defined as those with intermediate or high AD by NIA-Reagan criteria without other significant neuropathology, including brainstem, limbic or neocortical LBD, significant vascular disease or frontotemporal lobar degeneration (FTLD) [15]. Table 1 presents the clinical characteristics of the study participants including CDR, Braak score as well as CERAD score ($P<0.05$). Table 1 also presents the subject age (mean=81.0, $P=9.15$), sex distribution ($P=0.00037$) and RNA integrity number (RIN).

For comparison to a different brain region, an independent, publicly available, Accelerating Medicines Partnership–Alzheimer's Disease (AMP-AD) rRNA-depleted RNA seq data for inferior frontal gyrus tissue (BM44) generated by Mount Sinai Brain Bank (MSBB) (195 AD cases, 76 controls) was analyzed using the same pipeline (Supplementary Table 1). Additional hippocampus RNA-seq data of European ancestry generated by the Adult Changes in Thought (ACT) were downloaded from NIAGADS (25 AD cases and 50 Control) and analyzed using the same workflow (Supplementary Table 2).

CircRNA profiling/expression in the hippocampus and cortex of human aging/AD brains selects for circRNA from synaptic cognate genes

rRNA-depleted RNA from 210 hippocampi of subjects from ADRC were sequenced and evaluated for quality control. Samples with poor-quality RNA or outliers were excluded, leaving 207 samples for inclusion in the analysis. The resulting hippocampal sequencing data yielded an average of 45 million paired-end reads per individual. Reads were aligned to the human reference genome sequence (GRCh38) using STAR (version 2.6.1c) and CIRCexplorer3 was used to identify back-splice junctions and call circRNAs. As shown in Supplementary Table 3, in the hippocampus (BU ADRC dataset), 4,092 circRNAs from 2,056 unique gene locus were detectable (FPB>0 in >50% of the samples, FPB=fragments per billion mapped base). In the cortex BM44 region (MSBB AMP-AD dataset), 4,912 circRNAs were detectable from 2,414 unique gene locus with an average of 2 circRNA isoforms per gene. By applying the same pipeline, we detected high-confidence circRNAs from the other three MSBB cortical regions (BM10, BM22, BM36). 3,576 (66.7%) circRNAs were detected from all four MSBB brain regions (Supplementary Figure 1, Supplementary Tables 13 & 14), therefore, in the downstream analysis, MSBB BM44 was

selected as the primary cortex dataset, which is also consistent with what was previously reported [13].

Next, we selected for circRNAs that were widely expressed by selecting those circRNAs that exhibited expression in over 75% samples at FPB>0. More stringent expression thresholds progressively reduced the number of circRNA reaching significance. Application of this expression threshold reduced the number of circRNAs by more than 50% (2,147 and 2,722 in the hippocampus and cortex, respectively). At FPB>1, 308 hippocampal circRNAs and 975 cortical circRNAs were expressed in over 75% samples, and at FPB> 2 only 121 circRNAs were in the hippocampus vs. 508 in the cortex. The smaller fraction of highly expressed circRNAs observed in the hippocampus versus cortex might reflect the lower RNA quality in the hippocampal samples compared to the cortical samples. These findings are consistent with prior observations that the expression levels of non-coding RNAs including circRNAs are much lower than those of protein-coding mRNAs. All circRNAs expressed at >= 1 FPB in over 75% samples of hippocampus and cortex are listed in Supplementary Tables 4 and 5 in the online-only data supplement, respectively.

Gene ontology analysis of hippocampal circRNA showed that categories of synaptic and pre-synaptic localization and synaptic transmission were enriched in the 249 circRNA host genes expressed moderately (FPB>1 in over 75% samples) and 107 expressed highly (FPB>2) in the hippocampus (Supplementary Figure 2). In addition, we compared circRNAs detected from the hippocampus to MSBB BM44 cortex data. We found the percentage of commonly expressed circRNAs in both brain regions decreased, while the percentage of unique circRNAs in the cortex region increased (Supplementary Table 3).

Differential expression analysis to identify circRNA signatures for AD in the hippocampus and cortex

As shown above, a comparable number of circRNAs were detected at FPB>0 in the hippocampus (n=4,092) and in the cortex (n=4,912) with 80.5% (3,295/4,092) expressed in over 50% of both brain region samples. Therefore, for the differential expression (DE) analysis, we included circRNAs detected (FPB>0) across 50% of our BU ADRC hippocampus samples and MSBB BM44 cortex samples. Although more than one circRNAs was detected from each gene locus, for this study we selected the most abundant/significant circRNA from each gene locus. We obtained a total of 2,258 circRNAs, then meta-analyzed with the same circRNA transcripts in the MSBB-BM44 cortex dataset. At a false discovery rate (FDR) <0.05, we found 48 circRNAs (one circRNA per gene) differentially expressed between AD and controls (Table 2), with 9 circRNAs expressed only in the cortex. Among these, the expression patterns for 38 circRNAs were in the same direction for the hippocampus and BM44 cortex regions with 3 up-regulated and 35 down-regulated. Notably, circQKI was highly expressed (average FPB=2.3) and up-regulated in both AD brain regions (logFC=0.22, p=2.23 $\times 10^{-2}$ in cortex, and logFC=0.61, p=6.79 $\times 10^{-3}$ in hippocampus). circQKI is an RBP, reported to bind to the intron loop to regulate circRNA biogenesis in epithelial-mesenchymal transition tissue/cells (Figure 2A, B) [10]. circMAN2A1 was overexpressed in both AD brain regions although only significantly different in the cortex (Table 2), which might be due to the small number of control samples in our hippocampus

dataset. No circRNAs exhibiting significant differential expression between AD and control showed opposite disease-linked changes between the cortex and hippocampus.

We proceeded to check these 48 circRNAs in an independent hippocampus dataset (ACT). Among the set of 48 circRNA were 18 circRNAs detected (FPB>0) across 50% of the ACT samples. Three of the 18 circRNAs (MAPK9, RAPGEF5, NDST3) were significantly down-regulated in the AD hippocampus. circQKI was again expressed relatively highly (FPB=2.14) and up-regulated (logFC=0.44, p=0.015) in the AD hippocampus (see Supplementary Table 6 for 218 circRNAs at FDR<0.1 with results from all 3 datasets analyzed for AD status). Of note, circHOMER1, a neuronal-enriched circRNA abundantly expressed in the brain, was more abundant in the cortex compared to the hippocampus and down-regulated in AD across all three datasets with a similar fold change (logFC= −0.27 in the cortex, logFC= −0.28 in the two hippocampus datasets) (Figure 2A, B).

GO/KEGG enrichment analysis was performed using the corresponding host/cognate mRNA genes for the 218 differentially expressed circRNAs (FDR<0.1) (Figure 2C, Supplementary Table 7). The cognate mRNA transcripts showed significant enrichment for the synapse, postsynaptic density (17/e genes, FDR = 4.07e-06), synaptic vesicle membrane (8/209 genes, FDR=2.34e-03), axon and neuronal cell body (13/209 genes, FDR=2.71e-02) pathways. Further, enrichment for RNA processes and RNA splicing were observed among the 48 differentially regulated circRNAs (3/36 genes, FDR=8.76 e-05) (Figure 2C, Supplementary Table 7).

Top differentially expressed circRNAs correlate with AD pathology and cognitive loss/CDR in the hippocampus and cortex

Next, we sought to understand the relative importance of clinical and pathological outcomes in the association with circRNA expression patterns. circRNA expression was correlated with clinical dementia rating (CDR) and neuropathological AD-related traits including CERAD neuritic plaque score and Braak stage in both the hippocampus and cortex regions. CDR measures the severity of cognitive impairment ranging from no dementia (score=0) to severe dementia (score=1). Braak stages in AD are defined by the distribution of neurofibrillary tangles in the brain. Stages I and II involve confinement of neurofibrillary tangles to the transentorhinal region, the tangles spread to limbic regions in stages III and IV and the neocortex in stages V and VII. Neuritic plaque comprises amyloid-beta deposits and deteriorating neuronal material surrounding amyloid-beta deposits. CERAD neuritic plaque score ranges from 1 (definite AD) to 4 (no AD). As shown in Supplementary Table 8, most circRNAs were significantly associated with AD case status, dementia severity and neuropathological severity common to both hippocampus and cortex, while some circRNA showed phenotypic correlations that were selective for the cortex or hippocampus.

For 48 circRNAs differentially expressed between AD and normal control brains (FDR<0.05), we checked their association with Aβ pathology, tau pathology and clinical symptom of dementia scores. As shown in Figure 3A, among 45 circRNAs with association results for CDR, CERAD and Braak score, 69% (31/45) circRNAs were significantly associated with all three traits, 37/45 correlated with cognition (CDR), 42/45 correlated with Braak score, and 39/45 correlated with plaque Aβ-load (CERAD). More

AD-associated circRNAs correlated between CDR and Braak than CDR and Plaque (80% vs. 71%), indicating the critique role of Braak/tau-load with clinical diagnosed dementia stage and neuropathologically confirmed dementia stage. In addition, 6.7% (3/45) circRNAs exhibited an expression pattern correlating with Aβ pathology, while 13.3% (6/45) circRNAs exhibited an expression pattern correlating with tau pathology. Similar patterns were observed for 218 circRNAs differentially expressed between AD and control (Supplementary Figure 3). For selected circRNAs (circRIMS1, KCNN2, PSMB1, ATRNL1, PDE4B, HOMER1), scatterplots of their expression in hippocampus and cortex vs. CDR/Plaque/Braak are shown in Figure 3B. Each of these circRNA shows a significant correlation with Braak and CDR scores in the cortex. The cognate linear transcripts are associated with synaptic functions for *RIMS1*, *KCNN2* and *HOMER1* [16, 17].

The pattern of circRNA differential expression in AD cases is modified by the presence of vascular or Lewy body pathology (AD+VaD, AD+LBD)

Patterns of circRNA expression were examined from a range of dementia cases, including AD, Lewy body disease (LBD) and vascular dementia (VaD). Cases of AD frequently show multiple types of pathology, such as vascular pathology and Lewy body pathology. To explore the impact of other pathologies on circRNAs we identified circRNAs expressed differently between normal controls and AD patients exhibiting pathology for vascular dementia (AD+VaD) or Lewy body dementia (AD+LBD). As shown in Figure 4A, at $P<0.05$, only 39 circRNA exhibited differential expression that was common to all three disease conditions compared to controls, which was the smallest group of circRNAs studied. Far more circRNA exhibited expression patterns that were sensitive to pathological subtypes. 82 circRNAs showed differential expression in cases of pure AD or AD, while 62 circRNAs showed differential expression patterns that were unique in AD+VaD. Interestingly, the AD+LBD group exhibited the largest number of unique differentially expressed circRNAs (n=154), even though the number of AD+LBD patients (n=47) was smaller than pure AD (n=79) and AD+VaD (n=56). This larger number of differential circRNAs associated with AD+LBD could reflect more severe neuropathological features or a stronger association with synaptic pathology; however, the small sample size of the AD+LBD might increase the rate of false positives. Synaptic pathology is a strong pathway for circRNAs and also a strong pathway for α-synuclein, which is the predominant aggregated protein in Lewy bodies. Examining correlations with CDR instead of disease presence (AD only) did not increase the number of circRNAs identified that exhibited differential expression patterns common among disease subvariants. Although more circRNAs are associated with CDR (n=284) compared to disease presence (AD only, n=194), only 20 circRNAs were found common among AD+VaD, AD+LBD and CDR (Figure 4B). Comparison to plaque or tangle pathology yielded similarly small amounts of overlap. Correlations with plaque pathology yielded only 14 circRNAs that were common among AD+VaD, AD+LBD (Figure 4C), while correlations with neurofibrillary tangle pathology (Braak score) yielded only 30 circRNAs that were common among AD+VaD, AD+LBD (Figure 4D). Interestingly, the largest circRNA group observed (716 circRNAs) were circRNAs exhibiting differential expression correlating with plaque pathology (Figure 4C). These results suggest that the expression of circRNA varies according to the type

of neuropathology, perhaps reflecting differences in the underlying molecular regulatory pathways.

Analysis of circRNA for cognate AD-related GWAS genes or loci

To explore circRNA related to pathways most closely linked to AD, we examined circRNA for cognate genes with reported AD-related GWAS gene loci [18]. As shown in Figure 5, circPICALM is overexpressed in the hippocampal region of AD brains (P=0.033, logFC = 0.31). Analysis of cortical BM44 tissues revealed multiple circRNAs that were differentially expressed between AD and control cases for cognate genetically linked AD gene loci, including circPICALM (P-value = 0.019, logFC = 0.21), circPSEN1(P = 0.025, logFC = 0.20), which were both upregulated in AD, and circAPP (P=0.0152, logFC = −0.21), which was down-regulated in AD. The corresponding cognate linear mRNA levels were not altered by AD status, demonstrating that the AD-associated circRNA changes in expression were independent of AD-associated changes in cognate mRNA levels.

RT-qPCR validation

RT-qPCR was done to validate differentially regulated circRNA in the cortex and hippocampus regions. The samples used for validation were from an independent sample set collected from the AD Research Centers at Boston University and Emory University (Cortex, Brodmann 41-42: N=20 AD, N=20 Ctrl; Hippocampus: N=18 AD, N=8 Ctrl; details in the Supplementary Tables 9, 10). The qPCR data studies used two internal controls; GAPDH and circN4BP2L2. circN4BP2L2 (hsa_circ_0000471) was chosen specifically because it is a circRNA and has also been previously reported as a stable internal control for 22 human cell lines [19]; both informatics and qPCR analyses of our datasets (logFC=0.14, p=0.20 in the hippocampus; logFC=−0.003, P=0.99 in the cortex) confirmed the stability of circN4BP2L2 among the AD and control cases.

The 12 circRNAs were selected for validation based on high levels of expression in the cortex or hippocampus; the circRNA validated with qPCR were the same isoforms identified in the meta-analysis of BU and MSBB RNA sequencing datasets. Analysis of circRNA with high expression levels decreased the number of PCR cycles required for detection, which therefore reduced the associated variance. The circRNAs amplified were confirmed using Sanger sequencing. Validation of disease-linked changes using GAPDH for normalization was observed for 8 out of the 11 circRNA studied in the cortex, and 5 out of 12 samples studied in the hippocampus (for the hippocampus a “trend level of significance” was used for validation because of the smaller sample size) (Figure 6A, B). circKATNAL2 (hsa_circ_0108513) was significantly downregulated in both regions (Figure 6A, B). circKCNN2 (hsa_circ_0127664), circPSMB1(hsa_circ_0078784), circMAPK9 (hsa_circ_0001566) showed significant downregulation in the cortex and a trend level decrease in the hippocampus samples. Multiple other circRNA showed differences in cortical samples that were significant and validated however did not show validation in the hippocampus (likely because of smaller sample sizes); these circRNA included: circRIMS1 (hsa_circ_0132250), circRAPGEF5 (hsa_circ_0001681), circHOMER1 (hsa_circ_0006916), circATRNL1 (hsa_circ_0020093), circPDE4B (hsa_circ_0008433). qPCR plots normalized to circN4BP2L2 also gave similar results (Supplement Figure 4).

We also used qPCR to validate circRNA produced from AD-associated genes, using cortical samples as a basis for the validation studies. The circAPP (hsa_circ_0003038) showed significant downregulation using either the GAPDH or circN4BP2L2 for normalization (Figure 6C, Supplement Figure 4E). The circPSEN1 (hsa_circ_0003848) also showed a significant disease-linked increase in expression using circN4BP2L2 but not GAPDH as normalization control (Supplementary Figure 4E). Finally, we also examined the expression of circSLC8A1 which has been linked to Parkinson's disorder [20]. circSLC8A1 exhibited downregulation in the MSBB BM44 dataset (log FC=−0.27, p=0.004). qPCR of circSLC8A1 showed a strong and significant downregulation in the cortex of AD cases.

Of note, among the circRNA validated with qPCR, circATRNL1 is significantly associated with all three pathological traits. circHOMER1 and circPSMB1 are associated with CDR and Braak. circPSEN1 is significantly associated with plaque, however, interestingly we find its expression is restricted to the cortex. For Braak pathology, a correlation with circKCNN2 was observed.

microRNA binding sites in circRNA

Next, we examined the microRNA (miR) binding sites on the validated circRNA (Supplementary Table 12). We hypothesized that changes in the expression of the circRNA might lead to differential availability of miRNA. To these this hypothesis, we selected 3 miRs that are linked to AD and for which there were consensus sequences enriched in the validated circRNA data sets [21, 22] [23, 24]; we then tested whether changes in the circRNA levels correlated with changes in abundance of miR targets, which were chosen based on association with synapses and neurodegeneration (Figure 7A). We hypothesized that reduced circAPP in AD disease would increase the abundance of miR-15-5p resulting in the inhibition of target expression. Analysis of five miR-15-5p targets by qPCR (20 AD, 20 Ctrl) showed reduced target transcripts in AD, reaching a trend level of significance for 4 out of 6 transcripts examined (Figure 7B). Reduced circSLC8A1 in AD might increase the abundance of miR-7-5p, which would also inhibit target gene expression. qPCR analysis of 7 target transcripts (20 AD, 20 Ctrl) showed 6 out of 7 transcripts reduced in AD at a trend level of significance (Figure 7C). Finally, increased circPSEN1 in AD might reduce the availability of miR-137, which would also increase target gene expression. 2 out of 3 transcripts examined showed significantly increased expression (Figure 7D).

Neuronal exposure to oligomeric tau recapitulates disease-linked changed in circRNAs

Next, we investigated whether the changes in circRNA could be recapitulated in cell culture systems. We examined the expression of the validated circRNA in neuronal precursors cells (NPCs) differentiated from human iPSCs. Next, we extracted oligomeric tau (oTau, S1p fraction) from the brain of PS19 P301S 9month aged mice, as described previously [25–27]. The NPCs were treated with 80ng oligomeric tau (oTau) and harvested after 48 hrs, as described previously [26, 27], and qPCR was performed. As expected, oTau treatment of NPCs caused cytotoxicity (Supplementary figure 5A). The response of the NPCs to oTau was specific to some of the AD-associated targets. oTau treatment decreased expression of circAPP, circPDE4B, circRAPGEF5, circMAPK9, circRIMS1 and circATRNL1 (Figure 8A). Interestingly, circPSEN1 also showed a decrease in expression upon oTau treatment,

despite being upregulated in AD cases. circN4BP2L2 was tested as a negative control. To understand whether the circRNA differential regulation is specific to oTau treatment or induced by other stress responses, we subjected NPCs to oxidative stress using sodium arsenite. Interestingly, we observed no change in the expression of AD associated circRNA upon arsenite treatment (Supplementary Figure 5C), which demonstrates that some circRNA are selectively reduced in response to oTau treatment. Although acute treatment with sodium arsenite did not elicit a change in circRNA, the experimental design does not rule out the possibility that other types of stress might reduce levels of these circRNAs. Finally, we performed qPCR analysis on mRNA to investigate whether changes in circRNA induced upon oTau treatment correlate with changes in their cognate linear transcripts. The response of most circRNAs examined (5/7) paralleled the response of the cognate mRNAs (Figure 8B). However, circMAPK9 exhibited downregulation independent of its linear transcript; oTau induced a decrease in circMAPK9 but not linear MAPK9 mRNA (Figure 8A, B). In addition, circAPP and circPSEN1 were more responsive to oTau than linear *APP* and *PSEN1* mRNA (Figure 8A, B). This highlights that circMAPK9, circAPP and circPSEN1 regulation in response to oTau treatment is specific. Since circAPP showed a similar effect with oTau-treated NPCs as with AD cases, we further explored changes in circAPP-miRNA-15-5p-mRNA axis in NPCs. Out of four transcripts suggested to be regulated by miRNA 15-5p, we observed a decrease in *IGF1* and *SNAP25* expression (Figure 8C), which suggests dysregulation of similar biological pathways as in AD patients.

Discussion

CircRNAs comprise an important segment of the transcriptome that is particularly abundant in the brain, yet its contributions to neurodegenerative diseases are poorly understood. The pipeline that we established enables exploration of circRNA expression to identify those circRNA exhibiting the strongest changes with disease. Using this pipeline we identified 48 circRNA that exhibited differential expression between AD and control subjects. Examining the cortex, we observed that 10 out of 14 circRNA were subsequently validated by qPCR; the validation rate would potentially increase with a greater sample size.

CircRNAs are particularly interesting because they localize to 2 organelles critical to the disease process, synapses and stress granules (the latter being a membraneless organelle) [28, 29]. Dysfunction of circRNA biology in either of these organelles could directly impact the disease process. Indeed, a recent study of circRNAs identified in 5X-FAD mice identified a circRNA, Cwc27, that is increased with the disease [30]. Conversely, knockdown of Cwc27 reduced Aβ accumulation by sequestering the RNA binding protein Pur-α in the cytoplasm, and (importantly) increasing the expression of neprilysin [30]. The circRNAs that we observed are notable for the disease linkage and brain distribution. Our study employs the newest pipelines for circRNA identification and is also the first to examine the hippocampus, which is the region most affected in AD. The circRNAs that we identified showing the strongest DE linked to AD exhibited patterns of DE expression that correlated with indices of tauopathy (Braak staging) and cognitive loss (CDR) suggesting that these circRNAs reflect neuronal biology, which is consistent with the current understanding of circRNA functions. Interestingly, the DE circRNAs that we observed did not show DE for the corresponding mRNA, which raises the possibility that

the biology of circRNA either more directly contributes to or is more sensitive to the pathophysiology of AD.

Our evidence suggests that changes in circRNA could impact levels of free miRNAs, which would result in compensatory changes in cognate RNAs. We did indeed observe supportive data for over half the cognate mRNAs corresponding to targets of each miRNA examined, which is consistent with regulation by the expected miRNAs. However, the overlap of regulated mRNA/miRNA components was not complete. This is perhaps not surprising. The lack of full overlap between cognate mRNA expected to be targets of particular miRs and the actual mRNA targets assessed in our sample might reflect competition with other factors regulating transcript expression.

In order to understand the regulation of disease-linked circRNAs, we examined circRNA expression in NPCs. The first observation of note was the higher level of expression of the circRNAs in human NPCs versus HEK 293 cells, which we speculate reflects the neurobiology of neurons. The increase in circRNA expression occurring with the differentiation of NPCs supports a hypothesis that neuronal phenotypes lead to higher circRNA expression. The downregulation of the validated circRNAs following treatment with oTau highlights the responsiveness of circRNAs in NPC to regulation and suggests that oTau elicits regulation of circRNAs that is similar between NPCs and the brain. These observations also raise the possibility that some of the changes in circRNA expression in the AD brain might reflect the response to oTau toxicity. This observation would be consistent with Cervera-Carles et al, who noted similar responses of circRNAs between FTD-tau (but not FTD-TDP-43) and AD [16]. Future studies will now be able to explore the mechanisms through which oTau regulates circRNA production.

Strengths and Limitations: The strengths of this study derive from the application of the latest algorithms to the study of human brain, the examination of multiple brain regions and the extension of this work to NPCs, which provides a potential model for studying the regulation of circRNAs. However, the study also has important limitations. The small number of hippocampal samples limited the power of these investigations, with a resulting reduced ability to detect significant disease-linked changes using hippocampal samples. Another weakness is the correlational nature of the studies. Future studies will need to focus on modulating levels of circRNA to determine whether circRNA species can impact on the pathophysiology of AD.

Conclusion

CircRNAs are a novel class of regulatory RNAs but their role in AD pathogenesis is just beginning to be explored. Our study identified 48 circRNAs whose expression is linked to AD and are correlated with indices of tauopathy and cognitive loss in the cortex and hippocampus. Three of these molecules, circAPP, circPSEN1 and circMAPK9, stand out because in the brain they are regulated independently of the changes in the corresponding linear transcripts and because all three exhibit strong responses to treatment of NPCs with oligomeric tau, suggesting that these circRNA are responsive to the pathophysiology of AD.

Methods

Generating and Quality Control of the BU-ADRC Hippocampus RNA-seq data

Frozen human brain hippocampal tissues were collected at the BU-ADRC. Tissue was obtained from a coronal section of the caudal hippocampus at the level of the lateral geniculate nucleus and including all hippocampal layers CA1-4, subiculum, and dentate gyrus. After RNA extraction, RNA was purified using RNeasy Mini Kits (Catalog No. 74134, Qiagen, Germany). The RNA integrity number was calculated using an RNA 6000 Pico assay on a Bioanalyzer 2100 (Agilent Technologies, USA). The extracted RNA was also quantified using the Quant-iT RNA assay (Catalogue no. Q33140, Invitrogen, USA) on a Qubit Fluorometer (Thermo Fisher Scientific). Selected high-quality RNA were shipped to the Genome Center at Yale University in New Haven. Total RNA quality was determined by estimating the A260/A280 and A260/A230 ratios on nanodrop. RNA integrity was determined by Agilent Bioanalyzer. rRNA was depleted using the Kapa RNA HyperPrep Kit with RiboErase (Catalog No. KR1351, Kapa Biosystems, USA). Following sample fragmentation, adapter ligation, and library amplification, 100bp paired-end strand-specific sequencing was performed on an Illumina NovaSeq according to Illumina protocols. All samples were randomly assigned to a sequencing pool before sequencing, and RNA extraction and sequencing library preparation were performed blind to neuropathological case–control status. The average number of raw sequencing reads per individual was 40M (details of RNA quality control, RNA-seq library preparation, and sequencing are in Supplementary Methods).

We received 222 paired FASTQ files for 211 subjects of our BU-ADRC hippocampus samples. All datasets were subjected to three levels of quality check: 1) FastQC was used to inspect the initial fastq files that visually reflect sequencing quality and mismatching of sex (http://www.bioinformatics.babraham.ac.uk/projects/fastqc/). Low-quality reads (5% of the total) and poor-quality base were eliminated and adaptor sequences were trimmed using Trimmomatic (version 3.9)[31]. which is a fast, multithreaded command-line tool for trimming, cropping, and removing adapters from Illumina fastq data. 2)The percentage of mapped and unmapped reads was evaluated. 3) Qualification analysis of the aligned results was performed by a) checking the library size and gene expression level distribution for sample quality check and duplicate samples detection; b) checking sex marker gene expression level across all samples; c) PCA analysis for identifying hidden batch effects. One sample was identified as a duplicate and was excluded.

Preprocessing two public AD brain RNA-seq datasets

The Mount Sinai Brain Bank (MSBB) cortex RNA-seq dataset was downloaded from the Synapse portal (syn315774). In short, four different cortical regions were generated, which are the frontal pole (Brodman area (BM10), superior temporal gyrus (BM22), parahippocampal gyrus (BM36), and inferior frontal gyrus tissue (BM44)) from 315 individuals. The Ribo-Zero rRNA Removal Kit (Illumina human/mouse/rat) was applied to remove the rRNAs. The sequencing libraries preparation used TruSeq RNA Sample Preparation kit v.2. Using the Illumina HiSeq 2500, rRNA-depleted, 101-nucleotide, single-end, and non-stranded RNA-seq data were obtained from these libraries. In this study, only

MSBB BM44 cortex data were analyzed. For the MSBB data sample filter, we first excluded the samples that show “OKay” in the Action column in MSBB metadata (10 samples were excluded) and selected the unique samples for each subject and region (27 samples with duplicated sequencing data were excluded). This led to the selection of 271 unique samples (308-10-27=271) with good-quality of sequencing data to be included in this study. The sequence depth information and RNA quality of RIN and PMI values is included in Supplementary Table 15.

The Adult Changes in Thought (ACT) hippocampus RNA-seq dataset was downloaded from NIAGADS (NG00059, https://www.niagads.org/datasets/ng00059), which contains 25 AD cases and 50 normal controls. After rRNA-depletion, 51bp paired-end and stranded RNA-seq data were generated using the Illumina HiSeq 2500. After downloading the raw fastq files, the same preprocessing and quality check pipeline used above for our BU-ADRC Hippocampus RNA-seq data was applied to these two public AD brain RNA-seq datasets. The sequence depth information and RNA quality of RIN for the ACT dataset is included in Supplementary Table 16.

CircRNA detection and quantification using CIRCexplorer3-CLEAR

To detect circRNA from rRNA-depleted RNA-seq data, we implemented two different pipelines as shown in Figure 1. CIRCexplorer3-CLEAR is a pipeline designed for comparing the expression of circular and linear RNAs [32], which includes two main steps: alignment and quantification. The trimmed RNA-seq reads were firstly aligned to the human reference genome (GRCh38/hg38) using HISAT2 (version 2.0.5) [33] with known gene annotations for subsequent linear RNA quantification. HISAT2-mapped fragments were used to quantify and select the maximally-expressed transcript of a given gene using StringTie (version 1.3.3). FPB (fragments per billion mapped base) value was applied to quantitate/normalize linear RNA expression by HISAT2-mapped fragments to splicing-junction sites of the maximally-expressed transcript annotation.

Separately, HISAT2-unmapped fragments were mapped to the same hg38 reference genome using TopHat-Fusion (version 2.0.12) [34] for subsequent circRNA quantification. Then, fragments mapped to back-splicing-junction sites were retrieved from TopHat-Fusion (version 2.3.6; *CIRCexplorer2 parse -f -t TopHat-Fusion*) [35] and normalized by totally mapped bases to obtain FPB values for circRNA quantification. circRNA were called for each sample separately and were manually combined as a data matrix for further analysis.

clear_quant -g hg38.fa \ -i hisat_index \ -j bowtie1_index \ -G hg38_ref_all2.gtf —Finally, the number of detected circRNAs were summarized by applying different cutoff, for example, FPB> 0, 0.1, 0.2, 0.5, or 1.0 in over 25%, 50%, 70%, or 100% of total samples. circRNAs with FPB>0 in over 50% of samples were selected for downstream differential expression analysis. For these selected circRNAs, the ratio of corresponding linear RNAs and circRNAs is great than 0.1 in at least 3 samples. Just like CIRCexplorer3, DCC has two main steps (details were presented in Supplementary Methods).

Identifying circRNAs differentially expressed between AD and control in the hippocampus and cortex

CircRNAs that were not expressed in more than 50% of the samples were excluded from the analysis. Differential expression analyses for CIRCexplorer3 calling circRNA between AD cases and control were performed using Limma [36]. The FPB circ matrix with log2(x + 0.5) transformation was compared between AD cases and controls using linear regression models adjusting for sex, age, RQN (RNA quality number), and library batch.

Before running "limma", CIRCexplorer3 circRNA counts in each sample were normalized by FPB. The normalized FPB values were taken log2(x + 0.5) transformation. Subjects with missing covariate data and disease subgroup information were excluded. Only circRNAs expressed in more than 50% of the samples were included in the DE analysis. In the model, technical differences (RQN/PMI, batch), age/ Age of Death (AOD), and sex were included as covariates.

After obtaining differentially expressed results of AD vs. control by running "limma" for hippocampus and BM44 data separately, we performed a meta-analysis of the differential summary statistic results of hippocampus and BM44 using METAL [37] under a fixed effects model. A statistical significance threshold was defined as FDR<0.05/0.1. Significant circRNA-related cognate genes were used for pathway enrichment analysis using EnrichR [38].

circRNA association analysis with AD neuropathology and related endophenotypes in hippocampus and cortex

In addition to traditional case-control analysis, we investigated the circRNA association with AD neuropathological stage including amyloid CERAD score, tau Braak score, and clinical dementia rate with each study. In the BU-ADRC hippocampus data, a low CERAD score means a high amyloid burden and vice versa. However, in the MSBB BM44 cortex data, plaque mean (PM) value was provided with a high PM value which indicates a high amyloid burden. Therefore, in the meta-analysis of amyloid plaque burden, the direction of the coefficient estimated from BU-ADRC hippocampus data was first reversed, then input to METAL.

circRNA differential expression analysis in AD and mixed AD in the hippocampus

For BU-ADRC hippocampus RNA-seq data, similar to circRNAs differential expression analysis between AD and normal controls, mixed AD with vascular dementia (VaD) or AD with Lewy Boby (LBD) were compared to control to discover unique and common circRNAs differential expression patterns with the same covariates included in the analytic model using limma.

Quantitative real-time PCR (qRT-PCR)

30mg of human brain tissue was homogenized in 1ml of TRIzol (Catalog No. 15596026, Thermofisher Scientific, USA). 200μl of chloroform was added to each sample and mixed well. The samples were centrifuged at 13,000rpm for 15 minutes at 4°C. The RNA in the upper aqueous layer was subjected to column-based purification using the Qiagen RNeasy

Plus mini kit (Catalog No. 74134, Qiagen, Germany). For RNase R treatment, 1ug of total RNA was treated with RNAase R (Catalog no. ab286929, Abcam, USA) as per the manufacturer's protocol and RNA was reextracted using the Qiagen RNeasy Plus mini kit. RNA was reversed transcribed using random hexamer primers with High-Capacity cDNA Reverse Transcription Kit (Catalog No. 4368814, Thermofisher Scientific, USA). For qPCR, a reaction mixture of 1µl cDNA, 0.2µM primers, and 2.5µl Ssoadvanced™ Universal SYBR (Catalog No. 1725720, Bio-Rad, USA) up to 5µl was prepared in triplicates for each sample. qPCR was performed in Quantstudio 12K Flex qPCR System (Thermofisher Scientific, USA). Divergent primers were used to amplify circRNA. However, in some instances, the primers amplified more than one isoform for the circRNA and hence specific isoforms were amplified using primers at the back-splice junction. The sequence of primers used for amplification are provided in Supplementary Table 11. The relative expression levels were quantified with $2^{-\Delta\Delta Ct}$ method and either GAPDH or circN4BP2L2 was used for normalization. For calculating statistical significance unpaired t-test was used. All statistical analysis was done using GraphPad Prism 9.

Cell culture treatments

Neuronal precursor cells (NPCs) were obtained from ATCC (Catalog no. ACS 5004, ATCC, USA). The cells were maintained in ATCC-NPC medium (Catalog no. ACS 3003, ATCC, USA) in a 37°C incubator containing 5% CO2. oTau oligomers were generated from the brain of 9-month-old PS19 P301S mice by the fractionation method described previously [25–27]. 60,000 cells were plated in each well of 24 well plate in triplicates for each condition. NPCs were treated with 80ng of oTau oligomers for 48hrs. Post-treatment, RNA was isolated from cells and the spent media was analyzed for cytotoxicity using CyQUANT LDH Cytotoxicity Assay Kit(Catalog no. C20300, Invitrogen, USA). For oxidative stress, NPCs were treated with 500µM of sodium arsenite for 1 hour [39]. The induction of oxidative stress was validated by the presence of stress granules in cells by immunofluorescence assay (Supplementary Figure 5B).

Supplementary Material

Refer to Web version on PubMed Central for supplementary material.

Acknowledgements

Brain tissues for this study were provided by the NIH NeuroBioBank, the Boston University Alzheimer's disease center (NIH grants AG50204517 and P30-AG13846) and the Goizueta Alzheimer's Disease Research Center (ADRC) of Emory University (P30 AG066511). Funding for this grant was provided by NIH: AG0772577 BW/XZ, AG056318 (BW), AG074591 (BW), AG061706 (BW), AG064932 (BW) and the BrightFocus Foundation (BW), and the 2021 Jack Spivack Excellence in Neuroscience at Boston University School of Medicine (XZ).

REFERENCES

[1]. Guerra BS, Lima J, Araujo B, Torres LB, Santos J, Machado D, et al. Biogenesis of circular RNAs and their role in cellular and molecular phenotypes of neurological disorders. Semin Cell Dev Biol. 2021;114:1–10. [PubMed: 32893132]

[2]. Zhang XO, Wang HB, Zhang Y, Lu X, Chen LL, Yang L. Complementary sequence-mediated exon circularization. Cell. 2014;159:134–47. [PubMed: 25242744]

[3]. Memczak S, Jens M, Elefsinioti A, Torti F, Krueger J, Rybak A, et al. Circular RNAs are a large class of animal RNAs with regulatory potency. Nature. 2013;495:333–8. [PubMed: 23446348]

[4]. Maass PG, Glazar P, Memczak S, Dittmar G, Hollfinger I, Schreyer L, et al. A map of human circular RNAs in clinically relevant tissues. J Mol Med (Berl). 2017;95:1179–89. [PubMed: 28842720]

[5]. Szabo L, Salzman J. Detecting circular RNAs: bioinformatic and experimental challenges. Nat Rev Genet. 2016;17:679–92. [PubMed: 27739534]

[6]. Piwecka M, Glazar P, Hernandez-Miranda LR, Memczak S, Wolf SA, Rybak-Wolf A, et al. Loss of a mammalian circular RNA locus causes miRNA deregulation and affects brain function. Science. 2017;357.

[7]. Sekar S, Liang WS. Circular RNA expression and function in the brain. Noncoding RNA Res. 2019;4:23–9. [PubMed: 30891534]

[8]. Hansen TB, Wiklund ED, Bramsen JB, Villadsen SB, Statham AL, Clark SJ, et al. miRNA-dependent gene silencing involving Ago2-mediated cleavage of a circular antisense RNA. EMBO J. 2011;30:4414–22. [PubMed: 21964070]

[9]. Ashwal-Fluss R, Meyer M, Pamudurti NR, Ivanov A, Bartok O, Hanan M, et al. circRNA biogenesis competes with pre-mRNA splicing. Mol Cell. 2014;56:55–66. [PubMed: 25242144]

[10]. Conn SJ, Pillman KA, Toubia J, Conn VM, Salmanidis M, Phillips CA, et al. The RNA binding protein quaking regulates formation of circRNAs. Cell. 2015;160:1125–34. [PubMed: 25768908]

[11]. Barrett SP, Salzman J. Circular RNAs: analysis, expression and potential functions. Development. 2016;143:1838–47. [PubMed: 27246710]

[12]. Tao M, Zheng M, Xu Y, Ma S, Zhang W, Ju S. CircRNAs and their regulatory roles in cancers. Mol Med. 2021;27:94. [PubMed: 34445958]

[13]. Dube U, Del-Aguila JL, Li Z, Budde JP, Jiang S, Hsu S, et al. An atlas of cortical circular RNA expression in Alzheimer disease brains demonstrates clinical and pathological associations. Nat Neurosci. 2019;22:1903–12. [PubMed: 31591557]

[14]. Ma N, Pan J, Ye X, Yu B, Zhang W, Wan J. Whole-Transcriptome Analysis of APP/PS1 Mouse Brain and Identification of circRNA-miRNA-mRNA Networks to Investigate AD Pathogenesis. Mol Ther Nucleic Acids. 2019;18:1049–62. [PubMed: 31786335]

[15]. Newell KL, Hyman BT, Growdon JH, Hedley-Whyte ET. Application of the National Institute on Aging (NIA)-Reagan Institute criteria for the neuropathological diagnosis of Alzheimer disease. J Neuropathol Exp Neurol. 1999;58:1147–55. [PubMed: 10560657]

[16]. Cervera-Carles L, Dols-Icardo O, Molina-Porcel L, Alcolea D, Cervantes-Gonzalez A, Munoz-Llahuna L, et al. Assessing circular RNAs in Alzheimer's disease and frontotemporal lobar degeneration. Neurobiol Aging. 2020;92:7–11. [PubMed: 32335360]

[17]. Li J, Sun Q, Zhu S, Xi K, Shi Q, Pang K, et al. Knockdown of circHomer1 ameliorates METH-induced neuronal injury through inhibiting Bbc3 expression. Neurosci Lett. 2020:135050. [PubMed: 32450188]

[18]. Bellenguez C, Kucukali F, Jansen IE, Kleineidam L, Moreno-Grau S, Amin N, et al. New insights into the genetic etiology of Alzheimer's disease and related dementias. Nat Genet. 2022;54:412–36. [PubMed: 35379992]

[19]. Zhong S, Zhou S, Yang S, Yu X, Xu H, Wang J, et al. Identification of internal control genes for circular RNAs. Biotechnol Lett. 2019;41:1111–9. [PubMed: 31428905]

[20]. Hanan M, Simchovitz A, Yayon N, Vaknine S, Cohen-Fultheim R, Karmon M, et al. A Parkinson's disease CircRNAs Resource reveals a link between circSLC8A1 and oxidative stress. EMBO Mol Med. 2020;12:e11942. [PubMed: 32715657]

[21]. Fernandez-de Frutos M, Galan-Chilet I, Goedeke L, Kim B, Pardo-Marques V, Perez-Garcia A, et al. MicroRNA 7 Impairs Insulin Signaling and Regulates Abeta Levels through Posttranscriptional Regulation of the Insulin Receptor Substrate 2, Insulin Receptor, Insulin-Degrading Enzyme, and Liver X Receptor Pathway. Mol Cell Biol. 2019;39.

[22]. Liu HY, Fu X, Li YF, Li XL, Ma ZY, Zhang Y, et al. miR-15b-5p targeting amyloid precursor protein is involved in the anti-amyloid eflect of curcumin in swAPP695-HEK293 cells. Neural Regen Res. 2019;14:1603–9. [PubMed: 31089060]

[23]. Dong LX, Bao HL, Zhang YY, Liu Y, Zhang GW, An FM. MicroRNA-16-5p/BTG2 axis affects neurological function, autophagy and apoptosis of hippocampal neurons in Alzheimer's disease. Brain Res Bull. 2021;175:254–62. [PubMed: 34217799]

[24]. He D, Tan J, Zhang J. miR-137 attenuates Abeta-induced neurotoxicity through inactivation of NF-kappaB pathway by targeting TNFAIP1 in Neuro2a cells. Biochem Biophys Res Commun. 2017;490:941–7. [PubMed: 28655611]

[25]. Apicco DJ, Ash PEA, Maziuk B, LeBlang C, Medalla M, Al Abdullatif A, et al. Reducing the RNA binding protein TIA1 protects against tau-mediated neurodegeneration in vivo. Nat Neurosci. 2018;21:72–80. [PubMed: 29273772]

[26]. Jiang L, Lin W, Zhang C, Ash PEA, Verma M, Kwan J, et al. Interaction of tau with HNRNPA2B1 and N(6)-methyladenosine RNA mediates the progression of tauopathy. Mol Cell. 2021;81:4209–27 e12. [PubMed: 34453888]

[27]. Jiang L, Ash PEA, Maziuk BF, Ballance HI, Boudeau S, Abdullatif AA, et al. TIA1 regulates the generation and response to toxic tau oligomers. Acta Neuropathol. 2019;137:259–77. [PubMed: 30465259]

[28]. You X, Vlatkovic I, Babic A, Will T, Epstein I, Tushev G, et al. Neural circular RNAs are derived from synaptic genes and regulated by development and plasticity. Nat Neurosci. 2015;18:603–10. [PubMed: 25714049]

[29]. Chen S, Zhang J, Zhao F. Screening Linear and Circular RNA Transcripts from Stress Granules. Genomics Proteomics Bioinformatics. 2022.

[30]. Song C, Zhang Y, Huang W, Shi J, Huang Q, Jiang M, et al. Circular RNA Cwc27 contributes to Alzheimer's disease pathogenesis by repressing Pur-alpha activity. Cell Death Differ. 2021.

[31]. Bolger AM, Lohse M, Usadel B. Trimmomatic: a flexible trimmer for Illumina sequence data. Bioinformatics. 2014;30:2114–20. [PubMed: 24695404]

[32]. Ma XK, Wang MR, Liu CX, Dong R, Carmichael GG, Chen LL, et al. CIRCexplorer3: A CLEAR Pipeline for Direct Comparison of Circular and Linear RNA Expression. Genomics Proteomics Bioinformatics. 2019;17:511–21. [PubMed: 31904419]

[33]. Kim D, Langmead B, Salzberg SL. HISAT: a fast spliced aligner with low memory requirements. Nat Methods. 2015;12:357–60. [PubMed: 25751142]

[34]. Kim D, Salzberg SL. TopHat-Fusion: an algorithm for discovery of novel fusion transcripts. Genome Biol. 2011;12:R72. [PubMed: 21835007]

[35]. Zhang XO, Dong R, Zhang Y, Zhang JL, Luo Z, Zhang J, et al. Diverse alternative back-splicing and alternative splicing landscape of circular RNAs. Genome Res. 2016;26:1277–87. [PubMed: 27365365]

[36]. Ritchie ME, Phipson B, Wu D, Hu Y, Law CW, Shi W, et al. limma powers differential expression analyses for RNA-sequencing and microarray studies. Nucleic Acids Res. 2015;43:e47. [PubMed: 25605792]

[37]. Willer CJ, Li Y, Abecasis GR. METAL: fast and efficient meta-analysis of genomewide association scans. Bioinformatics. 2010;26:2190–1. [PubMed: 20616382]

[38]. Kuleshov MV, Jones MR, Rouillard AD, Fernandez NF, Duan Q, Wang Z, et al. Enrichr: a comprehensive gene set enrichment analysis web server 2016 update. Nucleic Acids Res. 2016;44:W90–7. [PubMed: 27141961]

[39]. Wheeler JR, Matheny T, Jain S, Abrisch R, Parker R. Distinct stages in stress granule assembly and disassembly. Elife. 2016;5.

RESEARCH IN CONTEXT

Systematic review:

PubMed searches identified other publications addressing circRNAs in AD. These references support the associations of circRNAs with AD and are cited.

Interpretation:

Prior studies have explored circRNA expression only in the AD cortex; this is the first study to compare the expression of specific disease-linked circRNAs among two brain regions (cortex and hippocampus) and by dementia subtype. Importantly, this is also the first study to explore the regulation of AD-linked circRNAs, identifying specific circRNAs that are strongly downregulated by the treatment of NPCs with oligomeric tau. These findings suggest that circRNA could be a biomarker for AD and treating neuronal cells with oligomeric tau can recapitulate some of these changes.

Future directions:

These studies pave the way for an elucidation of the molecular mechanisms underlying disease-dependent regulation of circRNA. Future studies will investigate how circRNAs interface with other RNA regulatory elements (e.g., RNA-binding proteins and miRNAs) in disease.

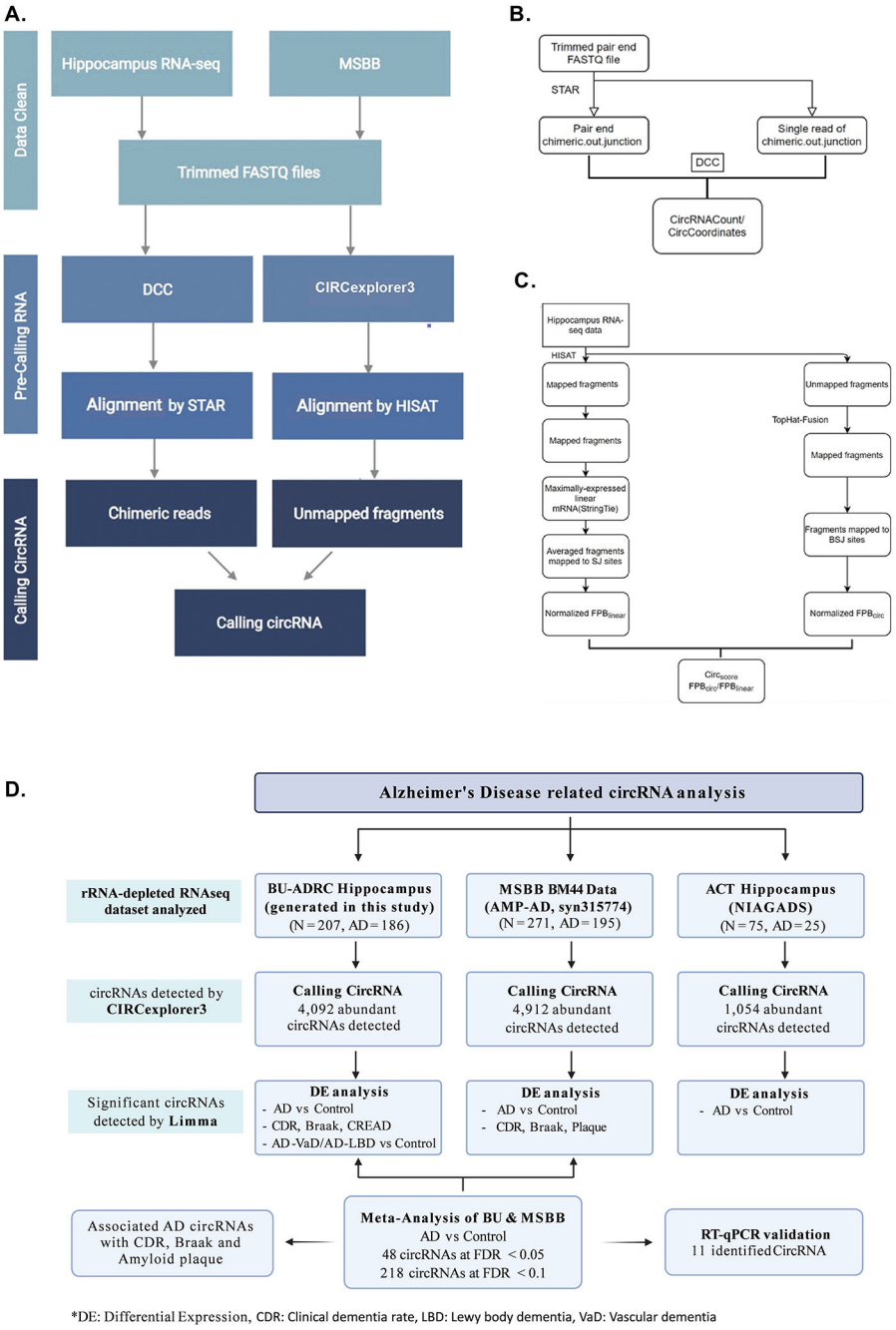

Figure 1. circRNA analysis workflow

(A) Workflow for circRNA calling. The hippocampus data and MSBB cortex region were used for analysis. Both DCC and circexplorer3 were used for calling but we represent only Circexplorer3 results and subsequent tables. (B) Pipeline for circRNA calling using DCC. (C) Pipeline for circRNA calling using Circexplorer3. (D) An overview of the pipeline used and results obtained for circRNA detection and differential expression analysis in three AD brain RNA-seq data.

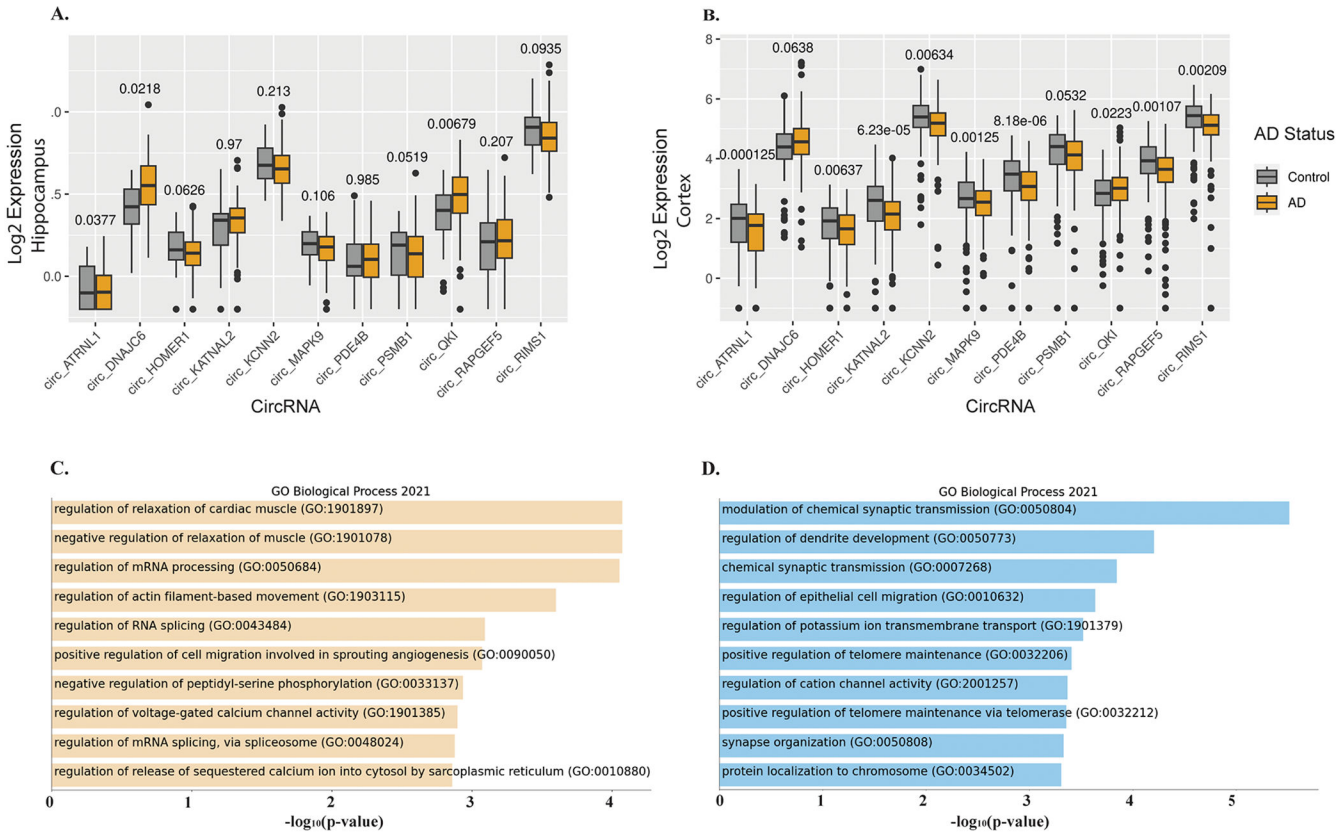

Figure 2. Top differentially regulated circRNAs between AD and control.

(2A-B) Boxplots showing the expression levels (represented as log2 transformed FPB) and distribution of top differentially regulated circRNA in the hippocampus (BU-ADRC) and BM44 cortex (MSSB AMP-AD), respectively. (**2C-D)** GO pathways enrichment analysis of cognate mRNA genes for 48 and 218 circRNAs, respectively that are differentially expressed at FDR<0.05 and FDR<0.1, respectively. P-value indicated on top of each boxplot.

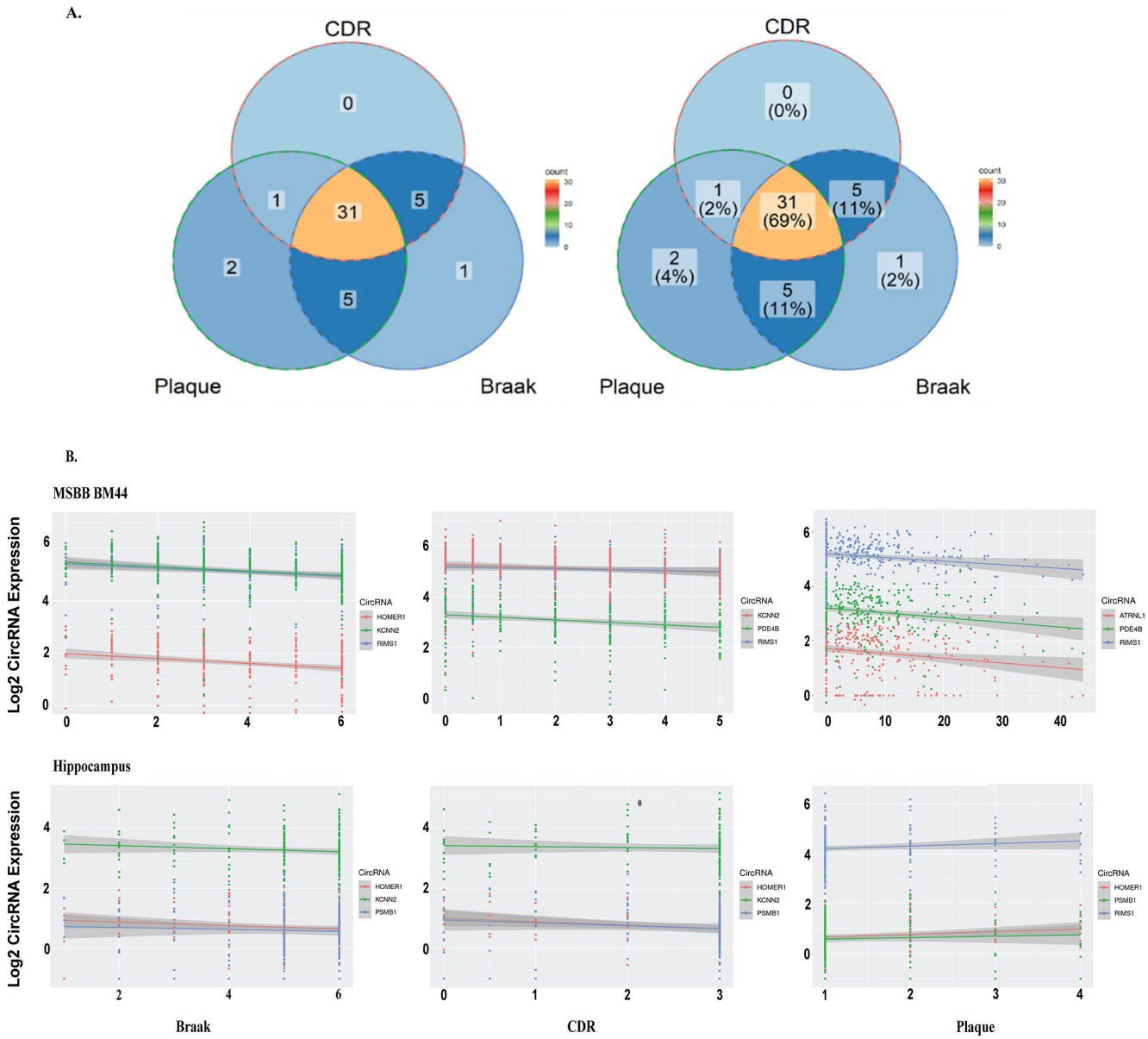

Figure 3. CircRNA associated with different indices of AD.

(A) Venn Diagram depicting the association of 48 DE circRNAs with AD pathology (Braak and Plaque) and CDR. (B) Scatter plot showing the association of Braak, CDR, and Plaque score with the top three significant circRNA. Coordinates are shown as color-coded dots for different kinds of circRNA and their correlation across subjects (within AD and control) is represented by fitted solid lines. Note, plaque mean score in MSBB BM44 is positively correlated with amyloid severity, but it is vice-versa in BU-ADRC hippocampus which is a CERAD score. For MSBB BM44 the corresponding R-values and P-values are as follow; Braak: HOMER1(−0.26, 3.40E-06), KCNN2(−0.33, 7.30E-09), RIMS1(−0.3,1.40E-07); CDR: KCNN2(−0.27, 1.50E-06), PDE4B(−0.26, 2.90E-06), RIMS1(−0.21,1.60E-04); Plaque: ATRNL1(−0.2, 5.50E-04), PDE4B(−0.24,1.70E-05), RIMS1(−0.28,6.90E-07). For hippocampus; Braak:

HOMER1(−0.15, 2.60E-02), KCNN2(−0.13, 7.00E-02), RIMS1(−0.032, 6.50E-01); CDR: HOMER1(−0.26, 5.00E-03), KCNN2(−0.11,2.30E-01), RIMS1(−0.2, 3.20E-02); Plaque: HOMER1(0.16, 2.30E-02), PSMB1(0.088,2.10E-01), RIMS1(0.1,1.30E-01).

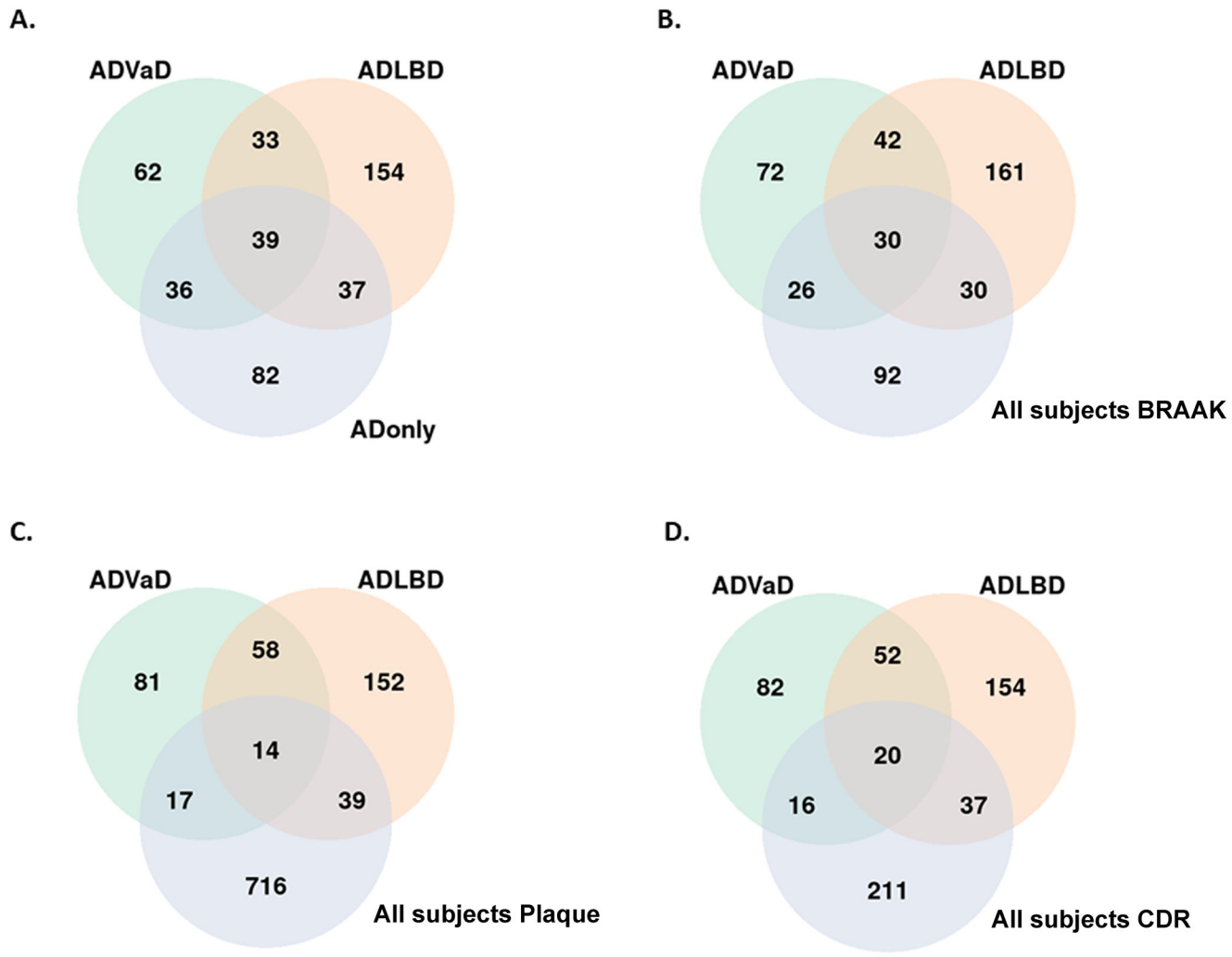

Figure 4. Venn diagram to depict differential expression analysis for AD subtypes in the hippocampus:

(A) Between ADVaD, ADLBD, and AD only cases. (B) Between ADVaD, ADLBD and circRNA correlated with Braak in all AD cases. (C) Between ADVaD, ADLBD and circRNA correlated with Plaque in all subjects. (D) Between ADVaD, ADLBD and circRNA correlated with CDR in all subjects.

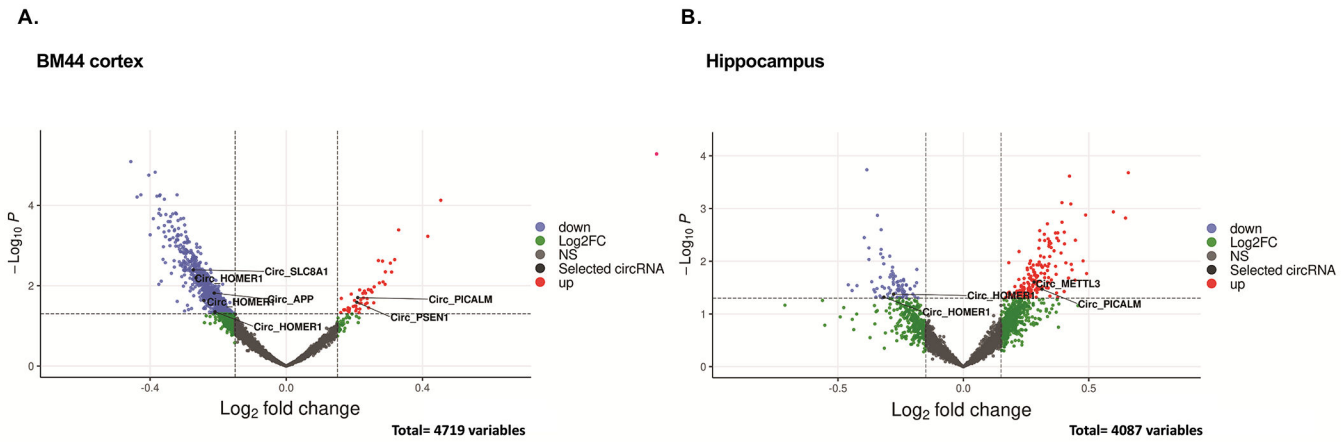

Figure 5. CircRNAs for known AD GWAS loci (*APP, PSEN1, PICALM*).

(A, B) Volcano plots of circRNAs differentially expressed in AD vs Control in Cortex and Hippocampus brain region, respectively. P-values were generated by empirical Bayes moderated test-test in limma. CircRNAs with a log-fold change > 0.15 and a −log10 adjusted P value of ≥1.3 (indicated with dashed lines) were considered significantly (red dots). Highlighted are the circRNA derived from AD-associated genes.

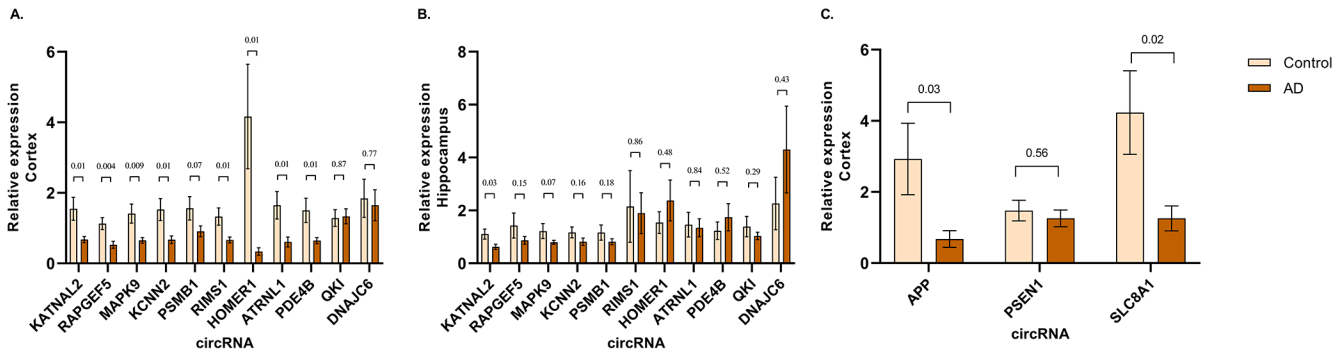

Figure 6. circRNA expression validation by RT-qPCR.

(A and B) Relative expression of 12 circRNA checked in the cortex (N=20 AD, 20 Ctrl) and hippocampus (N=18 AD, 8 Ctrl), (C) Relative expression of circRNA associated with AD loci in the cortex. Data are given as mean ± SE. P-value indicated on top of each bar.

A.

AD associated circRNA	Potential miRNA target	mRNA targets	Biological pathways associated with mRNA
circAPP	miR -15-5p	*IGF1, SNAP25, BDNF, TUBA4A, EIF4E*	Synapse, stress granule/ribonucleoprotein granules, vesicle trafficking
circSLC8A1	miR-7-5p	*GABRA1, SCNA, PFN2, G3BP2, RBFOX1, OXR1, EIF4E*	Synapse, stress granule/ribonucleoprotein granules, vesicle trafficking Oxidative stress
circPSEN1	miR-137	*NFATC1, EGFR1, NOTCH1*	Cell signaling, vesicle trafficking

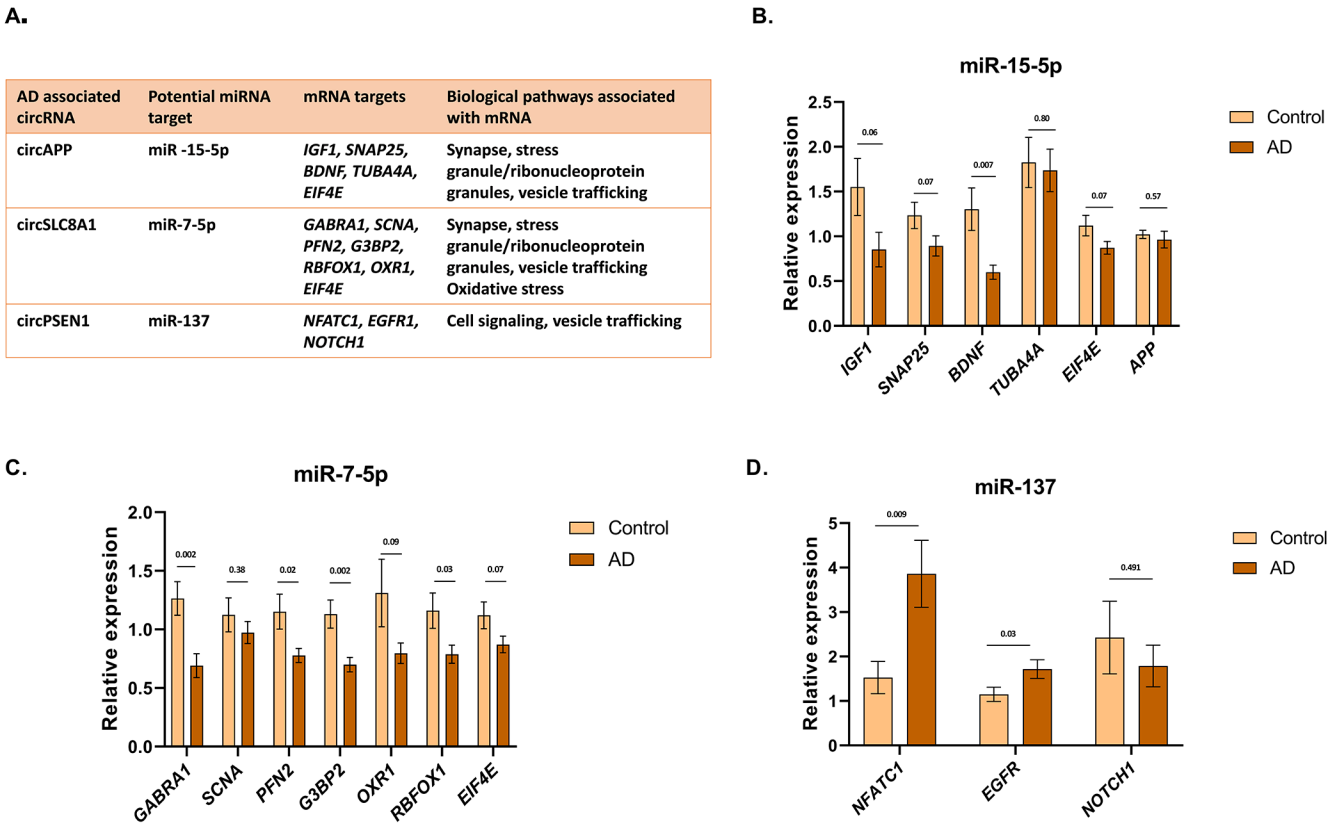

Figure 7. circRNA-miRNA-mRNA network analysis

(A) Table summarizing the circRNA-miRNA-mRNA network and biological pathways related. (B) Relative expression of linear transcript regulated by circAPP-miR-15-5p. (C) Relative expression of linear transcript regulated by circSLC8A1-miR-7-5p. (D) Relative expression of linear transcript regulated by circPSEN1-miR-137. Cortex samples (N=20 AD, 20 Ctrl). Data are given as mean ± SE. P-value indicated on top of each bar.

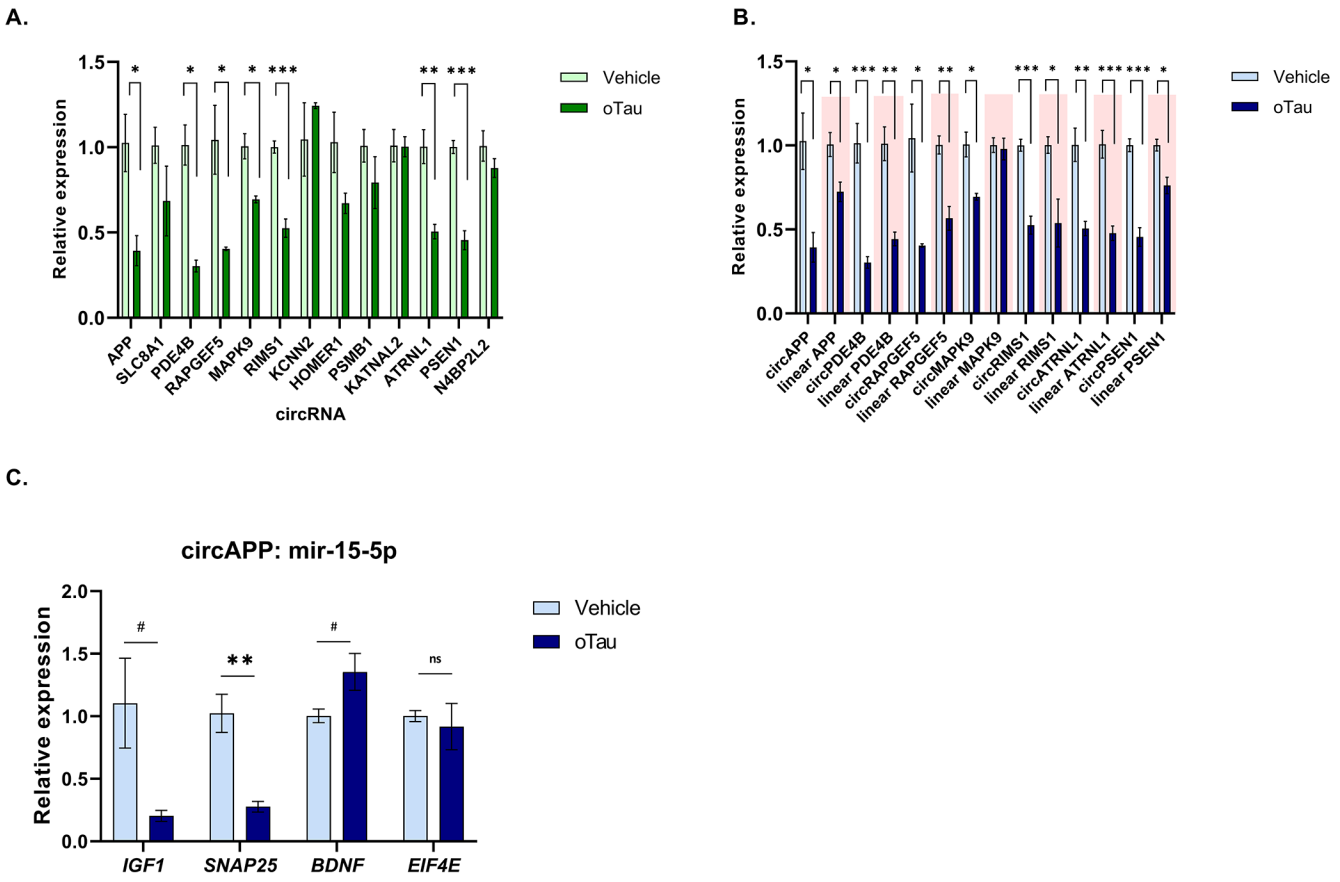

Figure 8. circRNA expression upon oTau treatment

(A) Relative expression of AD associated circRNA in NPCs with vehicle and oTau treatment. (B) Relative expression of cognate linear transcripts of circRNA modulated with tau toxicity in NPCs. (C) Relative expression of linear transcript regulated by circAPP-miR-15–5p. Data are given as mean ± SE, n = 3 biological replicates. $^{\#}$p<0.1 *p<0.05, **p<0.01, ***p<0.001

Table 1.

Distribution of subjects in BU-ADRC Hippocampus data including clinical and neuropathological measurement

Distribution of subjects in BU Hippocampus data (n=207)					
Variable	**AD_pure**	**AD+VaD**	**AD+LBD**	**AD other**	**Control**
N	79	56	47	4	21
Age(yr) (SD)	76.9 (8.30)	84.6 (9.70)	79.9 (5.85)	80.3 (5.56)	89.0 (9.00)
Female N (%)	12 (15.19)	17 (30.36)	7 (14.89)	0 (0)	10 (47.62)
RIN					
≤4.3	24	12	12	2	4
4.3<x≤5.6	18	19	14	1	1
5.6<x≤6.9	16	14	14	1	5
>6.9	21	11	7	0	11
CDR					
0	0	0	1	9	0
0.5	1	0	2	3	0
1	1	1	5	2	0
2	1	3	11	0	0
3	30	16	30	3	0
Braak					
1	0	0	0	0	4
2	0	0	0	0	11
3	1	3	2	0	5
4	3	5	5	3	0
5	26	21	17	1	1
6	49	27	23	0	0
CERAD					
0	0	0	0	0	0
1	70	46	39	3	2
2	7	7	8	1	2
3	2	3	0	0	8
4	0	0	0	0	9

N: sample size; RIN: RNA integrity number; SD: standard deviation. Values for Age and RIN are expressed as Mean ± SD. AD other was defined as the AD patients not defined as pure AD, AD+VaD, or AD+LBD.

Table 2.

Meta-analysis of circRNA differentially expressed between AD and controls in the hippocampus and cortex at FDR<0.05 (n=48).

circRNA		Meta results (BU+BM44)			BM44 Cortex (AD vs. Ctrl)			BU Hippocampus (pureAD vs.Ctrl)		
Coordinates (hg38)	Name	P. value	Dir	FDR	log2 FC	Ave Expr	P. Value	log2 FC	Ave Expr	P. Value
chr15:72760406-72775097	ADPGK	2.08E-07	−−	0.001	−0.35	1.00	2.54E-04	−0.47	−0.14	4.75E-05
chr5:59180594-59215968	PDE4D	6.29E-07	−−	0.001	−0.39	1.98	1.50E-05	−0.41	0.85	1.36E-02
chr14:46920011-47035304	MDGA2	5.37E-06	−−	0.005	−0.34	1.34	2.55E-04	−0.42	0.17	5.59E-03
chr10:115426249-115549536	ATRNL1	1.29E-05	−−	0.008	−0.37	1.82	1.25E-04	−0.33	−0.06	3.77E-02
chr7:66240324-66241270	TPST1	1.55E-05	−−	0.008	−0.37	0.54	1.75E-04	−0.28	−0.18	3.20E-02
chr1:9871186-9877989	CTNNBIP1	3.79E-05	−−	0.016	−0.32	0.56	5.50E-05	−0.18	−0.27	2.14E-01
chr2:106830065-106844034	ST6GAL2	4.45E-05	−−	0.016	−0.43	2.63	5.50E-05	−0.31	0.93	2.43E-01
chr10:92893348-92920050	EXOC6	5.83E-05	−?	0.019	−0.37	0.95	5.83E-05	NA	NA	NA
chr15:91251818-91268605	SV2B	6.70E-05	−−	0.019	−0.40	1.64	1.78E-05	−0.10	0.47	6.02E-01
chr10:21904521-21920963	DNAJC1	7.90E-05	−−	0.019	−0.34	1.13	1.89E-04	−0.17	−0.18	1.55E-01
chr7:157656356-157682937	PTPRN2	8.16E-05	−−	0.019	−0.34	0.20	7.03E-04	−0.30	−0.10	4.43E-02
chr8:53795646-53801896	ATP6V1H	9.60E-05	−−	0.020	−0.32	0.58	2.38E-04	−0.17	−0.34	1.53E-01
chrX:32287528-32348528	DMD	1.10E-04	−−	0.020	−0.32	1.64	7.26E-04	−0.36	0.93	6.01E-02
chr1:65913244-65918835	PDE4B	1.11E-04	−+	0.020	−0.46	3.11	8.18E-06	0.00	0.56	9.85E-01
chr2:2836918-2839025	AC011995.2	1.59E-04	−?	0.025	−0.37	1.10	1.59E-04	NA	NA	NA
chr1:585033-855380	AKT3	1.59E-04	−−	0.025	−0.30	0.95	4.57E-04	−0.20	0.37	1.40E-01
chr6:88844356-88891915	RNGTT	1.63E-04	−?	0.025	−0.33	0.55	1.63E-04	NA	NA	NA
chr13:100307191-100449305	PCCA	2.15E-04	−?	0.031	−0.39	0.63	2.15E-04	NA	NA	NA
chr6:61606289-61697253	KHDRBS2	2.34E-04	−−	0.031	−0.29	2.21	7.93E-04	−0.25	0.49	1.23E-01
chr4:30920152-30950215	PCDH7	2.39E-04	−−	0.031	−0.24	1.36	6.29E-03	−0.36	−0.01	8.63E-03
chr2:135709432-135710231	R3HDM1	3.07E-04	−−	0.034	−0.30	1.12	3.08E-04	−0.13	−0.04	3.38E-01
chr5:109767534-109823837	MAN2A1	3.12E-04	++	0.034	0.45	2.32	7.49E-05	0.10	2.37	7.40E-01
chr5:180261683-180280608	MAPK9	3.12E-04	−−	0.034	−0.30	2.54	1.25E-03	−0.23	0.86	1.06E-01
chr12:51684173-51689096	SCN8A	3.19E-04	−?	0.034	−0.36	0.82	3.18E-04	NA	NA	NA
chr6:68943829-69018499	ADGRB3	3.64E-04	−−	0.036	−0.33	1.03	4.02E-04	−0.13	−0.15	3.22E-01
chr4:61909559-61998265	ADGRL3	3.76E-04	−?	0.036	−0.32	0.70	3.75E-04	NA	NA	NA
chr5:11082695-11098748	CTNND2	3.87E-04	−−	0.036	−0.36	0.89	7.07E-05	−0.03	0.11	8.46E-01
chr20:41533049-41551360	CHD6	3.88E-04	−−	0.036	−0.27	1.61	1.89E-03	−0.23	0.64	8.66E-02
chr2:199308759-199381820	SATB2	4.05E-04	−−	0.036	−0.32	1.82	1.63E-04	−0.11	0.55	5.97E-01
chr6:72307257-72333835	RIMS1	4.58E-04	−−	0.038	−0.27	5.11	2.09E-03	−0.31	4.26	9.35E-02
chr9:98385639-98406141	GABBR2	4.61E-04	−?	0.038	−0.36	0.57	4.61E-04	NA	NA	NA
chr18:46946056-46946923	KATNAL2	4.70E-04	−−	0.038	−0.44	2.21	6.23E-05	−0.01	1.66	9.70E-01
chr8:80499493-80500382	ZBTB10	4.90E-04	−−	0.038	−0.28	0.80	2.41E-03	−0.24	0.04	8.61E-02
chr6:70732377-70798737	SMAP1	5.04E-04	−−	0.038	−0.29	1.06	1.39E-03	−0.20	0.22	1.56E-01

circRNA		Meta results (BU+BM44)			BM44 Cortex (AD vs. Ctrl)			BU Hippocampus (pureAD vs.Ctrl)		
Coordinates (hg38)	**Name**	**P. value**	**Dir**	**FDR**	**log2 FC**	**Ave Expr**	**P. Value**	**log2 FC**	**Ave Expr**	**P. Value**
chr7:22291174-22318037	RAPGEF5	5.27E-04	−−	0.039	−0.36	3.61	1.07E-03	−0.29	1.18	2.07E-01
chr8:135542653-135582073	KHDRBS3	5.50E-04	−−	0.039	−0.28	1.92	3.54E-03	−0.29	0.54	6.27E-02
chr6:54149055-54189914	MLIP	6.03E-04	−?	0.042	−0.35	1.66	6.03E-04	NA	NA	NA
chr1:83911164-83947282	TTLL7	6.13E-04	++	0.042	0.33	2.74	4.09E-04	0.14	1.17	4.73E-01
chr1:233198938-233236980	PCNX2	6.42E-04	−−	0.042	−0.26	2.34	1.42E-03	−0.21	1.05	1.95E-01
chr4:118105017-118143684	NDST3	6.48E-04	−−	0.042	−0.25	2.25	9.12E-03	−0.44	0.97	2.07E-02
chr7:43492074-43501322	HECW1	6.86E-04	−−	0.043	−0.33	1.09	1.55E-04	−0.04	0.14	8.27E-01
chr12:44665483-44714741	NELL2	7.12E-04	−?	0.043	−0.32	1.29	7.12E-04	NA	NA	NA
chr2:30459551-30568176	LCLAT1	7.18E-04	−−	0.043	−0.33	0.60	6.40E-04	−0.11	−0.06	4.00E-01
chr16:53254437-53274302	CHD9	7.57E-04	−−	0.044	−0.20	1.07	3.04E-02	−0.46	0.26	2.68E-03
chr7:18666212-18666476	HDAC9	7.78E-04	−−	0.045	−0.29	1.09	6.00E-04	−0.10	−0.21	4.44E-01
chr1:98953069-98956741	PLPPR5	8.42E-04	−−	0.047	−0.38	1.77	3.63E-04	−0.08	0.07	6.27E-01
chr7:14672928-14718685	DGKB	8.57E-04	−−	0.047	−0.29	0.58	1.62E-03	−0.18	−0.10	2.29E-01
chr6:163455278-163478896	QKI	8.84E-04	++	0.048	0.22	2.92	2.23E-02	0.61	2.36	6.79E-03

Dir: Direction, Ave Expr: Average Expression, FC: Fold change